International Journal of Applied Engineering Research ISSN 0973-4562 Volume 13, Number 7 (2018) pp. 4637-4651

Hall Current Effect on the MHD Flow of Newtonian Fluid through a Porous Medium

Pudhari Srilatha

Department of Mathematics, Institute of Aeronautical Engineering, Hyderabad, TS, India.

Abstract

In this paper, we discuss the hall current effect on the pulsatile flow of a viscous incompressible fluid through a porous medium in a flexible channel under the influence of transverse magnetic field using Brinkman's model. The non-linear equations governing the flow are solved using perturbation technique. Assuming long wavelength approximation, the velocity components and stresses on the wall are calculated up to order in $\mathcal{E}$ and the behavior of the axial and transverse velocities as well as the stresses is discussed for different variation in the governing parameters. The shear stresses on the wall are calculated throughout the cycle of oscillation at different points within a wavelength and the flow separation is analyzed.

Keywords: unsteady flows, hall current effects, pulsatile flows, porous medium

INTRODUCTION

The flow caused by a pulsatile pressure gradient through a porous channel or a porous pipe has been investigated in view of its applications in technological and physiological and physiological problems. In physiological fluid dynamics this model plays a significant role in explaining the dialysis of blood in artificial kidneys, vasomotor of small blood vessel such as arterioles, venues and capillaries. In most of the above investigations the boundary surface of the channel or pipe is assumed to have uniform cross section and an axial pressure gradient is maintained along the channel, which induces an unidirectional flow. In many biomedical problems one encounters the flow bounded by flexible boundaries and flow through uniform gap is only an approximation. Notable among them is the blood flow through veins.

A part from this, the non-Newtonian fluids are frequently encountered in food mixing, chyme movement in the intestine, blood flow at low shear rate, the flow of nuclear slurries, liquid metals and alloys. There are also situations where magnetic field characteristics in nonNewtonian fluids are significant. For instance, flow of mercury amalgams and lubrication with heavy oil and grease [3–9]. Current advances in the subject of Hall current involve Hall accelerators, nuclear power reactors, flight MHD and MHD generators. The Hall current IC switch or sensors are extremely useful to detects the presence or absence of a magnetic field and gives a digital signal for on and off. Large values of Hall current parameter in the presence of heavy-duty magnetic fields corresponds to Hall current, which is how, it shakes the current density and allows one to understand the impact of Hall current on the flow [10]. Hayat et al. [11] studied effects of Hall current on peristaltic flow of a Maxwell fluid in a porous medium. The effects of Hall current and heat transfer on MHD flow of a Burgers' fluid under the pull of eccentric rotating disks has been examined by Siddiqui et. al [12]. In another paper Gad [13], examined the effect of Hall currents on interaction of pulsatile and peristaltic transport induced flows for a particle-fluid suspension. Recently, studies [14–22] of heat and mass transfer in peristalsis have been considered by some researchers due to its applications in biomedical sciences. Heat transfer involves many complicated processes such as evaluating skin burns, destruction of undesirable cancer tissues, dilution technique in examining blood flow, paper making, food processing, vasodilation, metabolic heat generation and radiation between surface and its environment, metabolic heat generation and radiation between surface and its environment. It is clear from reviewing the existing literature, that no much attention has been given to the peristaltic flows with heat generation and Hall Currents, especially such attempts being further narrowed down for the case of non-Newtonian fluids. Recently, Krishna and M.G.Reddy [24] discussed the MHD free convective rotating flow of visco-elastic fluid past an infinite vertical oscillating plate. Krishna and G.S.Reddy [25] discussed the unsteady MHD convective flow of second grade fluid through a porous medium in a rotating parallel plate channel with a temperature-dependent source.Krishna and Swarnalathamma [26] discussed the peristaltic MHD flow of an incompressible and electrically conducting Williamson fluid in a symmetric planar channel with heat and mass transfer under the effect of an inclined magnetic field. Swarnalathamma and Krishna [27] discussed the theoretical and computational study of the peristaltic hemodynamic flow of couple stress fluids through a porous medium under the influence of a magnetic field with wall slip condition. Krishna and M.G. Reddy [28] discussed the unsteady MHD free convection in a boundary layer flow of an electrically conducting fluid through porous medium subject to uniform transverse magnetic field over a moving infinite vertical plate in the presence of heat source and chemical reaction. Krishna and G.S. Reddy [29] have investigated the simulation on the MHD forced convective flow through stumpy permeable porous medium (oil sands, sand) using Lattice Boltzmann method. Krishna and K.Jyothi [30] discussed the Hall effects on MHD Rotating flow of a visco-elastic fluid through a porous medium over an infinite oscillating porous plate with heat source and chemical reaction. B.S.K. Reddy et al.[31] investigated MHD flow of viscous incompressible nano-fluid through a saturating porous medium.

In this chapter we discuss the hall current effect on the pulsatile flow of a viscous incompressible fluid through a porous medium in a flexible channel under the influence of transverse magnetic field using Brinkman's model.

FORMULATION AND SOLUTION OF THE PROBLEM

Consider the unsteady fully developed pulsatile flow of viscous incompressible fluid through a porous medium in a flexible channel under the influence of transverse magnetic field of strength H_O. At $t>0$ the fluid is driven by a constant pressure gradient parallel to the channel walls. Choosing the Cartesian coordinate system O(x, y) the upper and lower walls of the channel are given by $y = \pm as\left(\frac{x}{\lambda}\right)$ Where, a is the amplitude, λ is the wavelength and s is an arbitrary function of the normalized axial co-ordinate $x^* = \frac{x}{\lambda}$. The entire flow is subjected to strong uniform transverse magnetic field normal to the plate in its own plane. Equation of motion along x-direction the x-component current density $\mu_e J_y H_o$ and the y-component current density $-\mu_e J_x H_o$. The equations governing the two dimensional flow of viscous incompressible fluid through a porous medium under the influence of transverse magnetic field, using Brinkman's model are

$$\frac{\partial u}{\partial x}+\frac{\partial v}{\partial y}=0 \tag{2.1}$$

$$\frac{\partial u}{\partial t}+u\frac{\partial u}{\partial x}+v\frac{\partial u}{\partial y} = -\frac{1}{\rho}\frac{\partial p}{\partial x}+\nu\left(\frac{\partial^2 u}{\partial x^2}+\frac{\partial^2 u}{\partial y^2}\right)+\mu_e J_y H_0-\frac{\nu}{k}u \tag{2.2}$$

$$\frac{\partial v}{\partial t}+u\frac{\partial v}{\partial x}+v\frac{\partial v}{\partial y} = -\frac{1}{\rho}\frac{\partial p}{\partial y}+\nu\left(\frac{\partial^2 v}{\partial x^2}+\frac{\partial^2 v}{\partial y^2}\right)-\mu_e J_x H_0-\frac{\nu}{k}v \tag{2.3}$$

Where (u, v) are the velocity components along O(x, y) directions respectively. ρ is the density of the fluid, p is the fluid pressure, k is the permeability of the porous medium, μ_e the magnetic permeability, ν the coefficient of kinematic viscosity and H_o is the applied magnetic field. Since the plates extends to infinity along x and y directions, all the physical quantities except the pressure depend on z and t alone. Hence u and v are function of z and t alone and hence the respective equations of continuity are trivially satisfied. When the strength of the magnetic field is very large, the generalized Ohm's law is modified to include the Hall current, so that

$$J+\frac{\omega_e\tau_e}{H_0}J\times H=\sigma\,(E+\mu_e\, q\times H) \tag{2.4}$$

Where, q is the velocity vector, H is the magnetic field intensity vector, E is the electric field, J is the current density vector, ω_e is the cyclotron frequency, τ_e is the electron collision time, σ is the fluid conductivity and μ_e is the magnetic permeability. In equation (2.4), the electron pressure gradient, the ion-slip and thermo-electric effects are neglected. We also assume that the electric field $E=0$ under assumptions reduces to

$$J_x+m\,J_y=\sigma\mu_e H_0 v \tag{2.5}$$

$$J_y-m\,J_x=-\sigma\mu_e H_0 u \tag{2.6}$$

where $m=\omega_e\tau_e$ is the hall parameter.

On solving equations (2.5) and (2.6) we obtain

$$J_x=\frac{\sigma\mu_e H_0}{1+m^2}(v+mu) \tag{2.7}$$

$$J_y=\frac{\sigma\mu_e H_0}{1+m^2}(mv-u) \tag{2.8}$$

Using the equations (2.7) and (2.8) the equations of the motion with reference to frame are given by

$$\frac{\partial u}{\partial t}+u\frac{\partial u}{\partial x}+v\frac{\partial u}{\partial y} = -\frac{1}{\rho}\frac{\partial p}{\partial x}+\nu\left(\frac{\partial^2 u}{\partial x^2}+\frac{\partial^2 u}{\partial y^2}\right)+\frac{\sigma{\mu_e}^2{H_0}^2}{\rho(1+m^2)}(mv-u)-\frac{\nu}{k}u \tag{2.9}$$

$$\frac{\partial v}{\partial t}+u\frac{\partial v}{\partial x}+v\frac{\partial v}{\partial y} = -\frac{1}{\rho}\frac{\partial p}{\partial y}+\nu\left(\frac{\partial^2 v}{\partial x^2}+\frac{\partial^2 v}{\partial y^2}\right)-\frac{\sigma{\mu_e}^2{H_0}^2}{\rho(1+m^2)}(v+mu)-\frac{\nu}{k}v \tag{2.10}$$

Eliminating p from equations (2.9) and (2.10), the governing the flow in terms of appropriate stream function ψ reduces to

$$(\nabla^2\psi)_t-\psi_y\nabla^2\psi_x+\psi_x\nabla^2\psi_y = -\left(\frac{\sigma\mu_e^2H_0^2}{\rho(1+m^2)}+\frac{\nu}{k}\right)\nabla^2\psi+\nu\nabla^4\psi \tag{2.11}$$

Where ∇^2 is the laplacian operator

The relevant conditions on ψ are

$$u = -\frac{\partial \psi}{\partial y}, v = \frac{\partial \psi}{\partial x} \tag{2.12}$$

The relevant boundary conditions are

$$\psi = 0,\ \psi_{yy} = 0 \qquad \text{on } y = 0 \tag{2.13}$$

$$\psi_y = 0,\ \psi = 1 + k_1 e^{it} \quad \text{on } y = s \tag{2.14}$$

An oscillatory time dependent flux is imposed on the flow resulting in a pulsatile flow we assume that oscillatory flux across the channel is $\psi_f\left(1 + k_1 e^{i\omega t}\right)$. Where ψ_f is the characteristic flux, k_1 is its amplitude and ω the frequency of oscillation. We define a characteristic velocity q corresponding to the characteristic flux ψ, so that ψ is $q\,a$.

We introduce the following non-dimensional variables.

$$x^* = \frac{\psi}{\lambda}, y^* = \frac{y}{a}, t^* = \omega t,\ \varepsilon = \frac{a}{\lambda}, \psi^* = \frac{\psi}{q\,a}, \psi^*_f = \frac{\psi_f}{q_a}$$

Substituting the above non-dimensional variables into the equation (2.11), the governing equation in terms of non-dimensional parameter ψ (on dropping the asterisks) reduces to

$$R\varepsilon\left(\varepsilon^2(\psi_x\psi_{yxx} - \psi_y\psi_{xxx}) + \psi_x\psi_{yyy} - \psi_y\psi_{xyy}\right) + S\varepsilon^2\psi_{tyy} + S\psi^4\psi_{txx} =$$

$$\varepsilon^4\psi_{xxxx} + \psi_{yyyy} + \varepsilon^2\left[2\psi_{xxyy} - \left(\frac{M^2}{1+m^2} + D^{-1}\right)\psi_{xx}\right] - \left(\frac{M^2}{1+m^2} + D^{-1}\right)\psi_{yy} \tag{2.15}$$

Where

$R = \frac{aq}{\nu}$ is the Reynolds number, $S = \frac{\lambda^2\omega}{\nu}$ is the oscillatory parameter, $D^{-1} = \frac{a^2}{k}$ is the inverse Darcy parameter, $M^2 = \frac{\sigma \mu_e^2 H_0^2 a^2}{\rho\nu}$ is the Hartmann number (Magnetic field Parameter), $m = \omega_e \tau_e$ is the hall parameter.

Equation (2.15) is highly non-linear and is not amenable for exact solution. However assuming the slope of the flexible channel ε small (<<1). We take ψ may be given asymptotic expansion in the form

$$\psi = \left(\psi_0 k_1 e^{it}\,\bar{\psi}_0\right) + \varepsilon\left(\psi_1 + k_1 e^{it}\,\bar{\psi}_1\right) + \text{------} \tag{2.16}$$

We are making use of transformation

$$\eta = \frac{y}{s(x)} \tag{2.17}$$

And the boundary conditions at $y = s(x)$, Now to be satisfied at $\eta = 1$.

Substituting equation (2.16) in the non-dimensional equation (2.15) and equating like powers of ε, the equations corresponding to the zeroth and first order steady and unsteady components are,

Zeroth order,

$$\frac{\partial^4\psi_0}{\partial y^4} - \left(\frac{M^2}{1+m^2} + D^{-1}\right)\frac{\partial^2\psi_0}{\partial y^2} = 0 \tag{2.18}$$

$$\frac{\partial^4\bar{\psi}_0}{\partial y^4} - \left(\frac{M^2}{1+m^2} + D^{-1}\right)\frac{\partial^2\psi_0}{\partial y^2} = 0 \tag{2.19}$$

First Order,

$$\frac{\partial^4\psi_1}{\partial y^4} - \left(\frac{M^2}{1+m^2} + D^{-1}\right)\frac{\partial^2\psi_1}{\partial y^2} = R\left[\frac{\partial\psi_0}{\partial x}\frac{\partial^3\psi_0}{\partial y^3} - \frac{\partial\psi_0}{\partial x}\frac{\partial^3\psi_0}{\partial x\partial y^2}\right] \tag{2.20}$$

$$\frac{\partial^4\bar{\psi}_1}{\partial y^4} - \left(\frac{M^2}{1+m^2} + D^{-1}\right)\frac{\partial^2\bar{\psi}_1}{\partial y^2} =$$

$$R\left[\frac{\partial\psi_0}{\partial x}\frac{\partial^3\bar{\psi}_0}{\partial y^3} + \frac{\partial\bar{\psi}_0}{\partial x}\frac{\partial^3\psi_0}{\partial y^3} - \frac{\partial\psi_0}{\partial y}\frac{\partial^3\bar{\psi}_0}{\partial x\partial y^2} - \frac{\partial\bar{\psi}_0}{\partial y}\frac{\partial^3\psi_0}{\partial x\partial y^2}\right] \tag{2.21}$$

Substituting (2.2.17) in equations (2.2.18) and (2.2.20) we obtain

$$\frac{\partial^4\psi_0}{\partial\eta^4} - \left(\frac{M^2}{1+m^2} + D^{-1}\right)s^2\frac{\partial^2\psi_0}{\partial\eta^2} = 0 \tag{2.22}$$

$$\frac{\partial^4\psi_1}{\partial\eta^4} - \left(\frac{M^2}{1+m^2} + D^{-1}\right)s^2\frac{\partial^2\psi_1}{\partial\eta^2} = Rs\left[\frac{\partial\psi_0}{\partial x}\frac{\partial^3\psi_0}{\partial\eta^3} - \frac{\partial\psi_0}{\partial\eta}\frac{\partial^3\psi_0}{\partial x\partial\eta^2}\right] \tag{2.23}$$

The corresponding boundary conditions to be satisfied are

$$\psi_0 = 0 = \frac{\partial^2\psi_0}{\partial\eta^2},\ \psi_1 = 0 = \frac{\partial^2\psi_1}{\partial\eta^2} \qquad \text{on} \qquad \eta = 0 \tag{2.24}$$

$$\frac{\partial\psi_0}{\partial\eta} = 0,\ \psi_0 = 1,\ \frac{\partial\psi_1}{\partial\eta} = 0,\ \psi_1 = 0 \qquad \text{on} \qquad \eta = 1 \tag{2.25}$$

Again substituting (2.17) in the equations (2.19) and (2.21) we obtain,

$$\frac{\partial^4 \bar{\psi}_0}{\partial \eta^4} - \left(\frac{M^2}{1+m^2} + D^{-1}\right) s^2 \frac{\partial^2 \bar{\psi}_0}{\partial \eta^2} = 0 \qquad (2.26)$$

$$\frac{\partial^4 \bar{\psi}_1}{\partial \eta^4} - \left(\frac{M^2}{1+m^2} + D^{-1}\right) s^2 \frac{\partial^2 \bar{\psi}_1}{\partial \eta^2} = Rs$$

$$\left[\frac{\partial \psi_0}{\partial x}\frac{\partial^3 \bar{\psi}_0}{\partial \eta^3} + \frac{\partial \bar{\psi}_0}{\partial x}\frac{\partial^3 \psi_0}{\partial \eta^3} - \frac{\partial \psi_0}{\partial \eta}\frac{\partial^3 \bar{\psi}_0}{\partial x \partial \eta^2} - \frac{\partial \bar{\psi}_0}{\partial \eta}\cdot\frac{\partial^3 \psi_0}{\partial x \partial \eta^2} \right] \qquad (2.27)$$

The corresponding boundary conditions to be satisfied.

$$\bar{\psi}_0 = 0 = \frac{\partial^2 \bar{\psi}_0}{\partial \eta^2},\ \bar{\psi}_1 = 0 = \frac{\partial^2 \bar{\psi}_1}{\partial \eta^2} \qquad \text{on} \qquad \eta = 0 \qquad (2.28)$$

$$\frac{\partial \bar{\psi}_0}{\partial \eta} = 0,\ \bar{\psi}_0 = 1,\ \frac{\partial \bar{\psi}_1}{\partial \eta} = 0,\ \bar{\psi}_1 = 0 \qquad \text{on} \qquad \eta = 1 \qquad (2.29)$$

Solving the equations (2.22) and (2.23) subjects to the boundary conditions (2.24) and (2.25) we obtain.

$$\psi_0 = C_1 \sinh(\sigma_1 \eta) + C_2 \eta \qquad (2.30)$$

$$\psi_1 = C_3 \sinh(\sigma_1 \eta) + C_4 \eta + C_5 \eta^2 \sinh(\sigma_1 \eta) + C_6 \eta \cosh(\sigma_1 \eta) + C_7 \sinh(2\sigma_1 \eta) \qquad (2.2.31)$$

Similarly solving equations (2.26) and (2.27) subjected to the corresponding boundary conditions (2.28) and (2.29).

$$\bar{\psi}_0 = C_8 \sinh(\sigma_1 \eta) + C_9 \eta \qquad (2.32)$$

$$\bar{\psi}_1 = C_{10} \sinh(\sigma_1 \eta) + C_{11} \eta + C_{12} \eta^2 \sinh(\sigma_1 \eta) + C_{13} \eta \cosh(\sigma_1 \eta) + C_{14} \sinh(2\sigma_1 \eta) \qquad (2.33)$$

Substituting equations (2.30), (2.31), (2.32) and (2.33) in the equation (2.16), we obtain

$$\psi = \left[C_1 \sinh(\sigma_1 \eta) + C_2 \eta\right] + k_1 e^{it}\left[C_8 \sinh(\sigma_1 \eta) + C_9 \eta\right] + \varepsilon\{\ C_3 \sinh(\sigma_1 \eta) + c_4 \eta +$$
$$C_5 \eta^2 \sinh(\sigma_1 \eta) + C_6 \eta \cosh(\sigma_1 \eta) + C_7 \sinh(2\sigma_1 \eta) + k_1 e^{it}(\ C_{10} \sinh(\sigma_1 \eta) +$$
$$+ C_{11} \eta + C_{12} \eta^2 \sinh(\sigma_1 \eta) + C_{13} \eta \cosh(\sigma_1 \eta) + C_{14} \sinh(2\sigma_1 \eta)\ )\ \} \qquad (2.34)$$

Using the equation (2.12), the axial velocity and the transverse velocity are given by

The axial velocity,

$$u = \frac{-1}{s(x)}\{\ (C_1 \sinh(\sigma_1 \eta) + C_2 \eta)_\eta + k_1 e^{it}(C_8 \sinh(\sigma_1 \eta) + C_9 \eta)_\eta +$$
$$+ \varepsilon\ (\ \left[(C_3 \sinh(\sigma_1 \eta) + C_4 \eta + C_5 \eta^2 \sinh(\sigma_1 \eta) + C_6 \eta\ \cosh(\sigma_1 \eta) + C_7 \sinh(2\sigma_1 \eta)\right]_\eta +$$
$$+ k_1 e^{it}\left[C_{10} \sinh(\sigma_1 \eta) + C_{11} \eta + C_{12} \eta^2 \sinh(\sigma_1 \eta) + C_{13} \eta\ \cosh(\sigma_1 \eta) + C_{14} \sinh(2\sigma_1 \eta)\right]_\eta\ )\ \}$$

and the transverse velocity,

$$v = (C_1 \sinh(\sigma_1 \eta) + C_2 \eta)_x + k_1 e^{it}(C_8 \sinh(\sigma_1 \eta) + C_9 \eta)_x +$$
$$+ \varepsilon\{\ \left[(C_3 \sinh(\sigma_1 \eta) + C_4 \eta + C_5 \eta^2 \sinh(\sigma_1 \eta) + C_6 \eta\ \cosh(\sigma_1 \eta) + C_7 \sinh(2\sigma_1 \eta)\right]_x +$$
$$+ k_1 e^{it}\left[C_{10} \sinh(\sigma_1 \eta) + C_{11} \eta + C_{12} \eta^2 \sinh(\sigma_1 \eta) + C_{13} \eta\ \cosh(\sigma_1 \eta) + C_{14} \sinh(2\sigma_1 \eta)\right]_x\ \}$$

Shear stress at the wall $y=s(x)$ is given by

$$\tau = \frac{\sigma_{xy}(1 - s_{xx}) + (\sigma_{yy} - \sigma_{xx}) s_x}{1 + (s_x)^2}$$

Where $\sigma_{xy} = -\mu(\psi_{yy} - \psi_{xx})$, $s(x) = 1 + \delta \sin x$, $\sigma_{yy} - \sigma_{xx} = 1 - 4\mu\psi_{xy}$

There are substituting for ψ_{yy} etc., we obtained the non-dimensional shear stress.

$$\therefore \tau = \frac{1}{s^2 A_1^2 (2 + (\delta \sin x)^2 + 2\delta \sin x)} \{ [(1 - \delta \sin x) A_1^2 .$$

$$\{ -\sigma^2 s^2 \sinh(\sigma s \eta).[\frac{1 + k_1 e^{it}}{A_1} + \varepsilon C_3 \delta \cos x + \varepsilon C_5 \eta^2 + \frac{2\varepsilon C_6}{\sigma s}]$$

$$- \varepsilon \sigma s \eta \cosh(\sigma s \eta).(4 C_5 \delta \cos x + C_6 (\sigma s)) -$$

$$- \varepsilon 2 C_5 \delta \cos x . \sinh(\sigma s \eta) - \varepsilon C_7 \sigma^2 s^2 \sinh(2\sigma s \eta) \}]$$

$$- [\left(4\varepsilon (1 + k_1 e^{it})(1 + \delta \sin x)\right) \times \{ \sigma \delta \cos x \sinh(\sigma s) [\cosh(\sigma s \eta)$$

$$(1 + \sigma^2 s^2) + \sigma s \eta \sinh(\sigma s \eta) - \cosh(\sigma s)]$$

$$- \sigma^2 s \delta \cos x \cosh(\sigma s)(\cosh(\sigma s \eta) + \sigma s \eta \sinh(\sigma s \eta) + \sigma^2 s \delta \cos x \}] \}$$

RESULTS AND DISCUSSION:

The flow governed by the non-dimensional parameters *R* the Reynolds number, D^{-1} inverse Darcy parameter, δ the amplitude of the boundary wave, k_1 the amplitude of oscillatory flux, *M* the magnetic parameter (Hartman number), *S* the oscillatory parameter and *m* hall parameter. The axial, transverse velocities and the stresses are evaluated computationally for different variations in the governing parameters *R*, D^{-1}, δ , k_1, *M*, *S* and *m*. For computational purpose we chose the boundary wave $s(x) = 1 + \delta \sin x$ in the non-dimensional form. The figures (1-16) represent the velocity components *u* and *v* for different variations of the governing parameters being the other parameters fixed. We observe that for all variations in the governing parameters, the axial velocity *u* attains its maximum on the mid plane of the channel. We notice that the magnitude of the axial velocity *u* enhances and the transverse velocity *v* reduces with increasing the Reynolds parameter *R*. The behavior of transverse velocity *v* is oscillatory with its magnitude decreasing on *R* increases through small values less than 30 and later reduces for further increase in *R*. The resultant velocity also enhances with increasing the Reynolds parameter *R* (Fig 1 and 2). From figures (3 and 4) we concluded that both the velocity components *u* and *v* reduces with increase in the inverse Darcy parameter D^{-1}. Here we observe that higher the permeability of the porous medium larger the axial velocity along the channel and rate of increase is sufficiently high. Similarly, the resultant velocity reduces with increasing in the inverse Darcy parameter D^{-1}. It is evident that the magnitude of *u*, *v* and the resultant velocity increase with increasing the parameters k_1, x and *m* (5, 6, 9, 10, 13 and 14). The magnitude of the axial velocity *u* enhances and the transverse velocity *v* decreases with increasing in the amplitude of the boundary wave δ . The resultant velocity also reduces with increasing the parameter δ (Fig 7 and 8). We notice that the magnitude of the velocity components *u* and *v* reduces with increasing the intensity of the magnetic field *M*. The resultant velocity also decreases with increasing the Hartmann number *M* (Fig 11 and 12). The magnitude of the axial velocity *u* enhances and the transverse velocity *v* reduces with increasing the oscillatory parameter *S*. The behavior of transverse velocity *v* is oscillatory with its magnitude decreasing on *S* increases through small values less than 3 and later reduces for further increase in *S*. The resultant velocity also enhances with increasing the oscillatory parameter *S* (Fig 15 and 16).

The shear stress on the upper wall with *S*=1 is evaluated through the entire cycle of oscillation at different points within a wave length for different sets of parameter δ . we choose the boundary wave as $s(x) = 1 + \delta \sin x$ in non-dimensional form. As already stated the criterion for the recognition of separation is the existence of a point at which the shear stresses at the wall less than or equal to zero throughout the entire cycle of oscillation. The influence of porosity in checking separation may be observed from table (1) for arbitrary values of *R*, D^{-1}, k_1, δ , *M* and *m*. This is evident that the shear stress on the upper wall does not vanish or become negative at any point in a wave length range throughout the entire cycle of oscillation. The magnitudes of the stresses enhance with increasing *R*, D^{-1}, k_1, *m* and *R* and reduces with increasing δ and magnetic parameter *M* being fixed *S*.

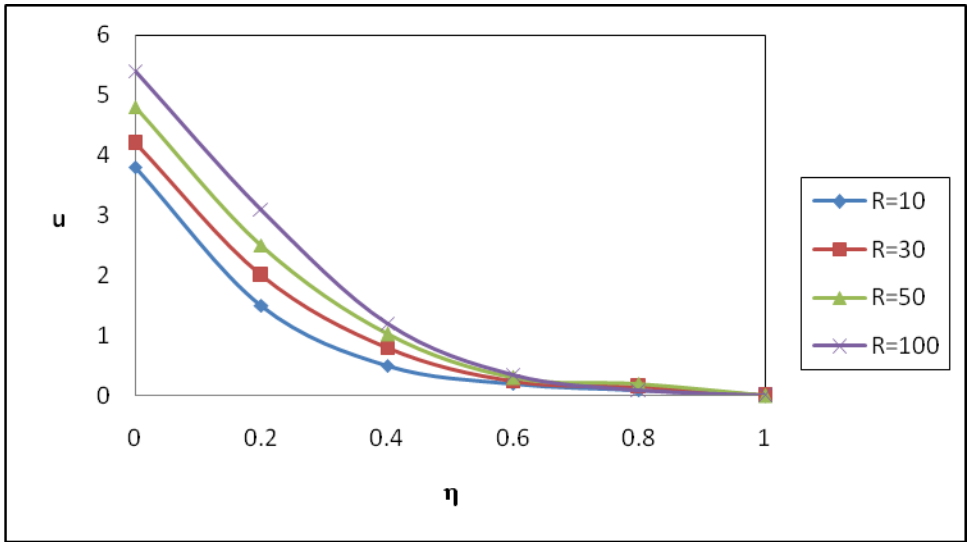

Figure 1: The velocity profile for u against R

k_1=1, S=1, D^{-1} =1000, M=2, m=1, $x = t = \frac{\pi}{4}$, $\delta = 0.01$

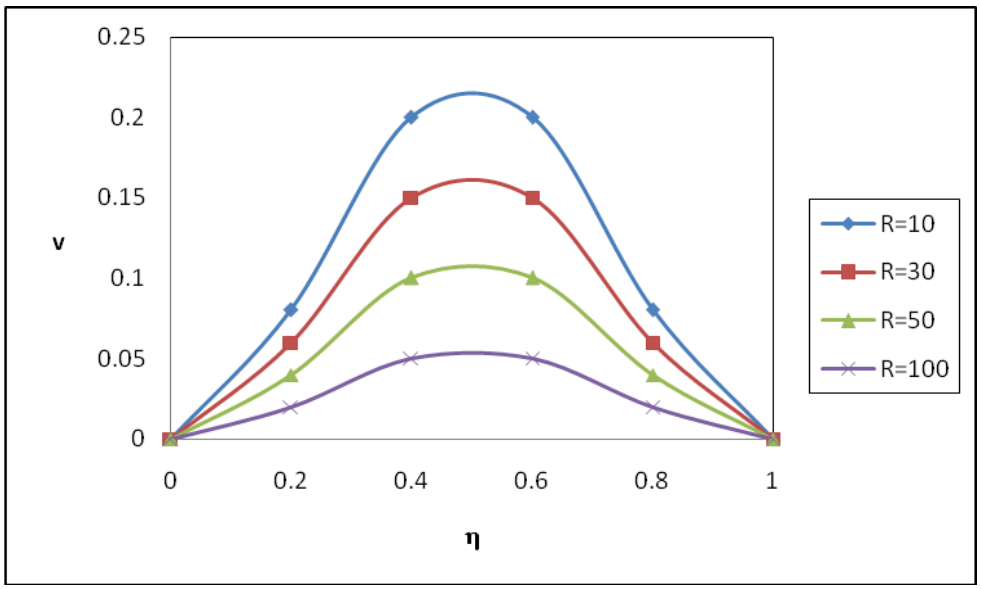

Figure 2: The velocity profile for v against R

k_1=1, S=1, D^{-1} =1000, M=2, m=1, $x = t = \frac{\pi}{4}$, $\delta = 0.01$

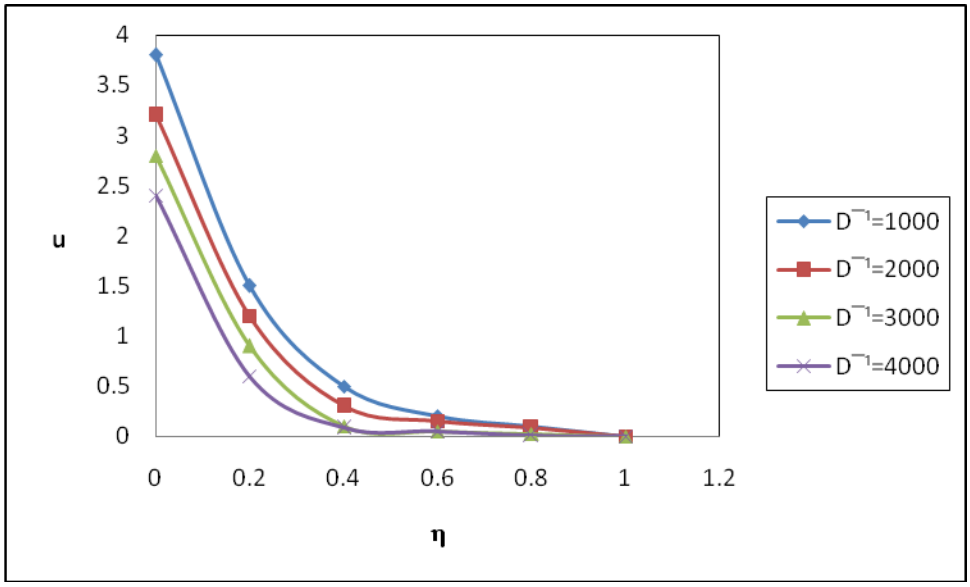

Figure 3: The velocity profile for u against D^{-1}

R=10, S=1, k_1=1, M=2, m=1 $x = t = \frac{\pi}{4}$, $\delta = 0.01$

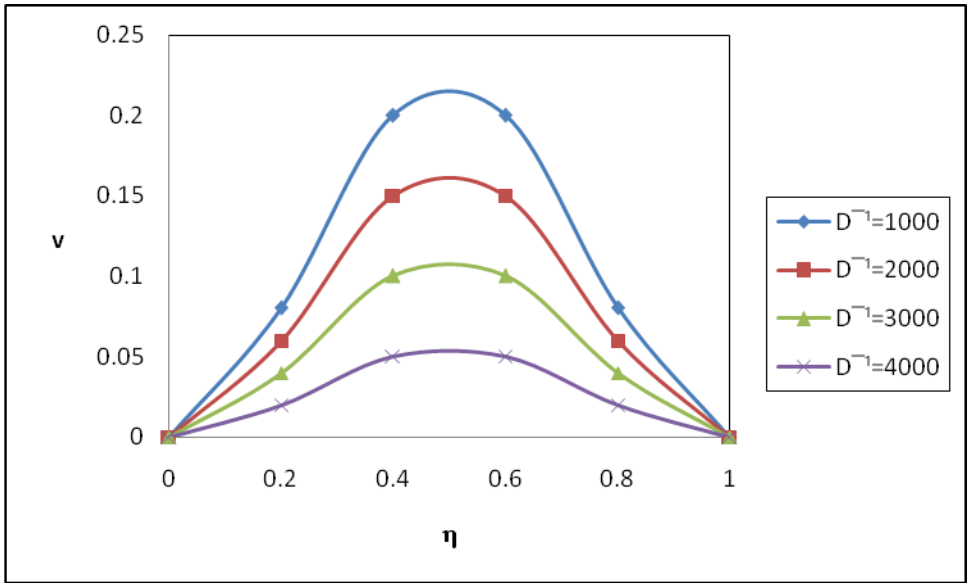

Figure 4: The velocity profile for v against D^{-1}

R=10, S=1, k_1=1, M=2, m=1 $x = t = \frac{\pi}{4}$, $\delta = 0.01$

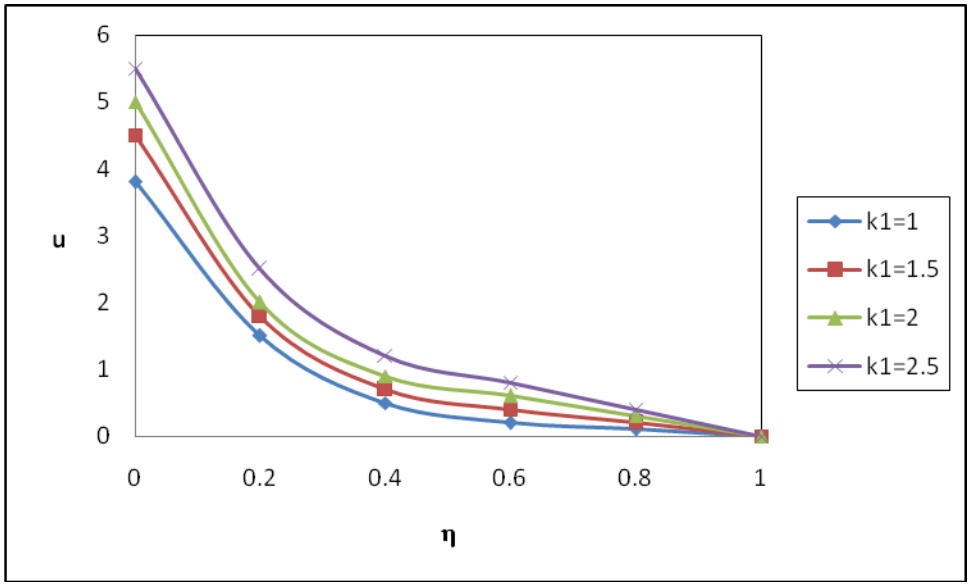

Figure 5: The velocity profile for u against k_1

m=1, S=1, D^{-1} =1000, M=2, $x = t = \frac{\pi}{4}$, R=10, $\delta = 0.01$

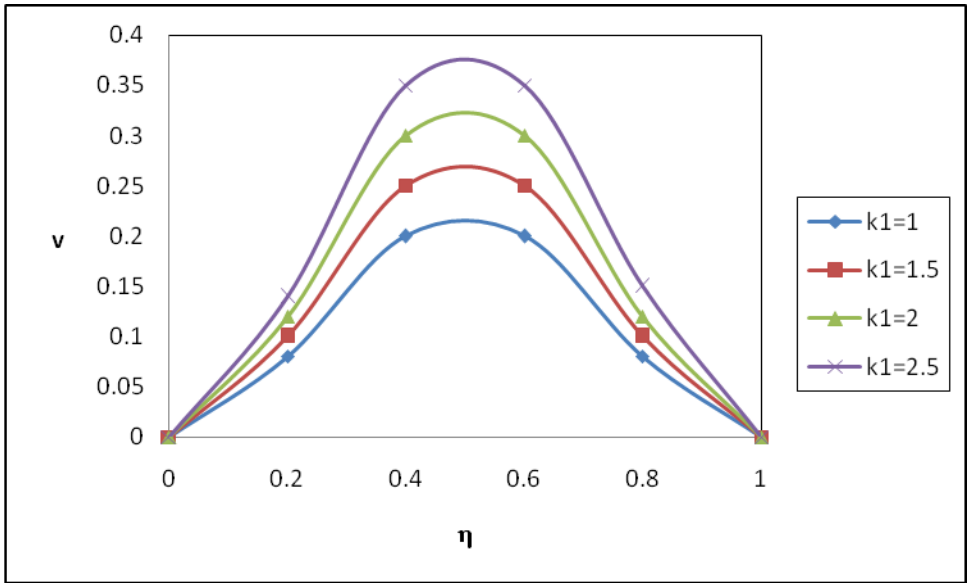

Figure 6: The velocity profile for v against k_1

m=1, S=1, D^{-1} =1000, M=2, $x = t = \frac{\pi}{4}$, R=10, $\delta = 0.01$

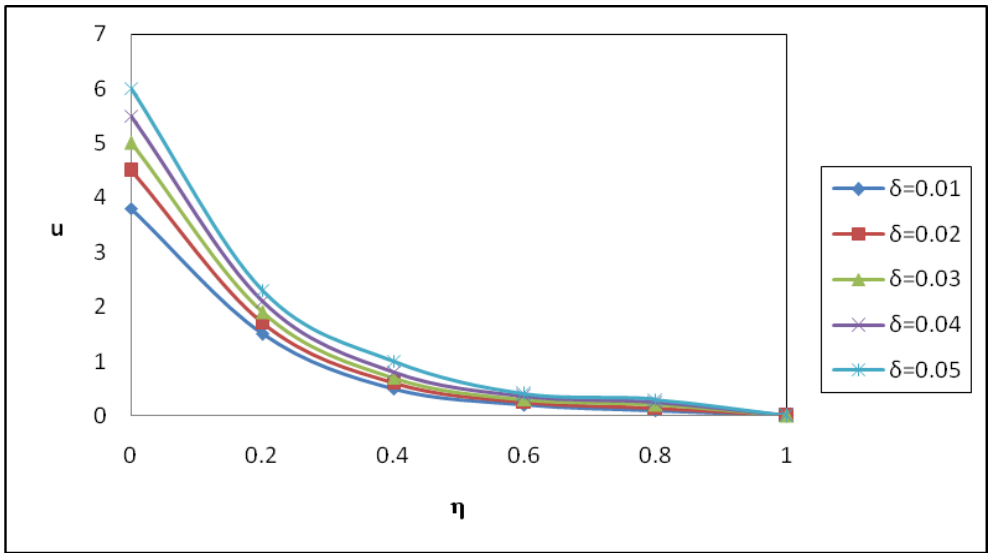

Figure 7: The velocity profile for u against δ

k_1=1, S=1, D^{-1} =1000, R=10, M=2, $x = t = \frac{\pi}{4}$, m=1

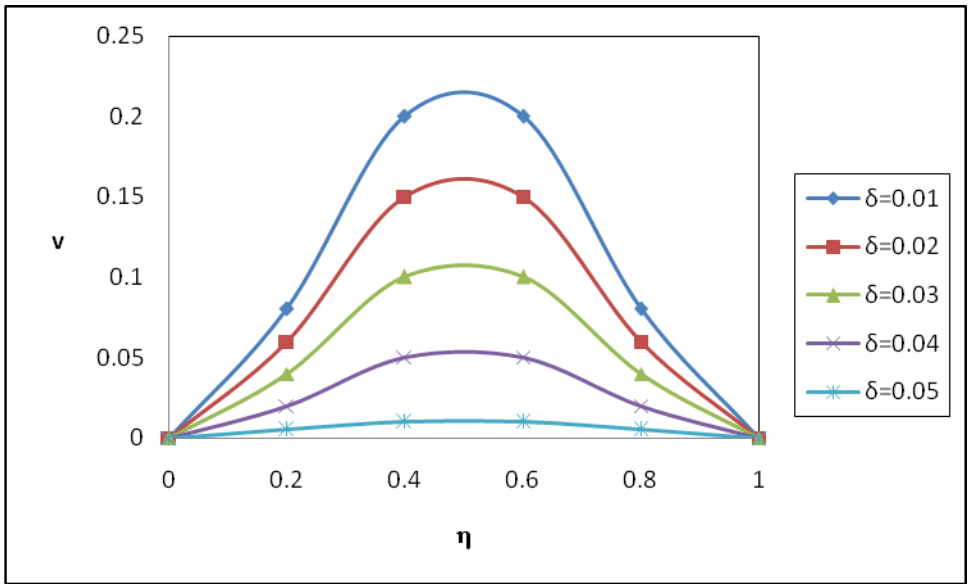

Figure 8: The velocity profile for v against δ

k_1=1, S=1, D^{-1} =1000, R=10, M=2, $x = t = \frac{\pi}{4}$, m=1

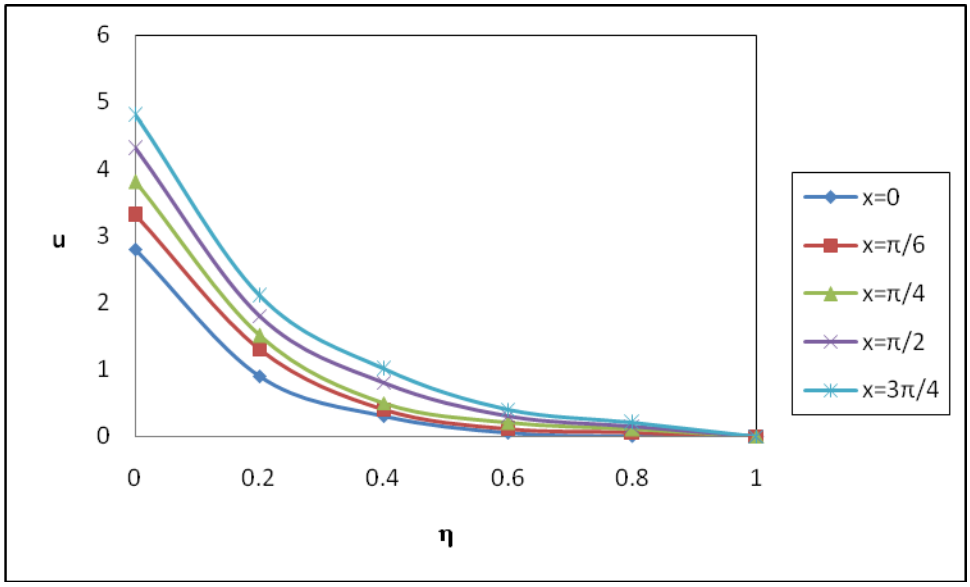

Figure 9: The velocity profile for u against x

R=10, S=1, D^{-1} =1000, k_1=1, M=2, m=1, $t = \frac{\pi}{4}$, $\delta = 0.01$

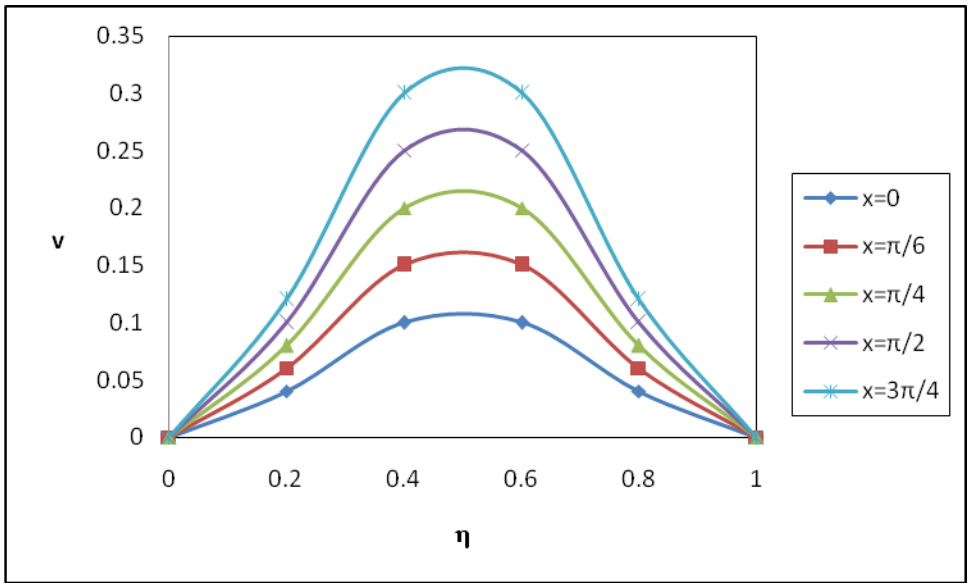

Figure 10: The velocity profile for v against x

R=10, S=1, D^{-1} =1000, k_1=1, M=2, m=1, $t = \frac{\pi}{4}$, $\delta = 0.01$

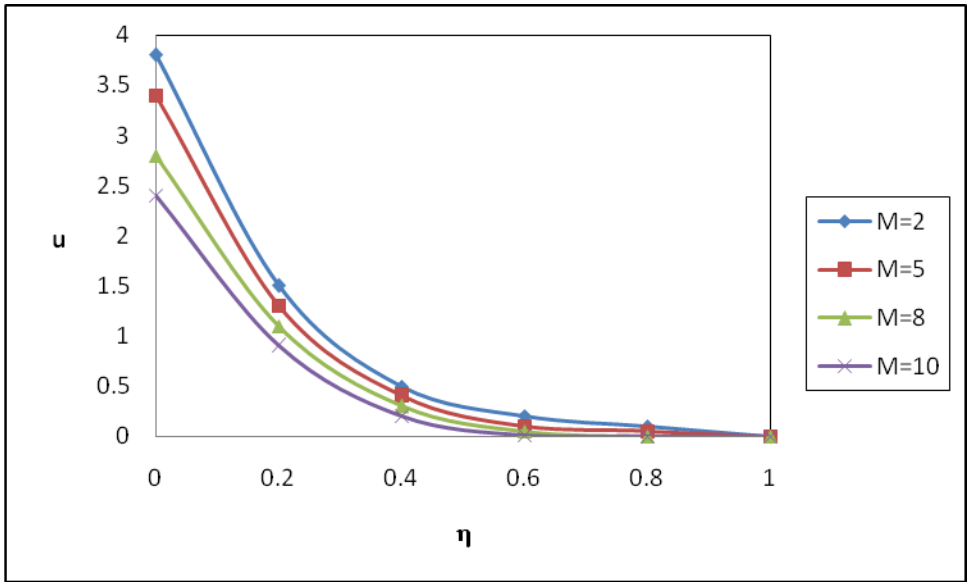

Figure 11: The velocity profile for *u* against M

k_1=1, *S*=1, D^{-1} =1000, *m*=1, $x = t = \frac{\pi}{4}$, *R*=10, $\delta = 0.01$

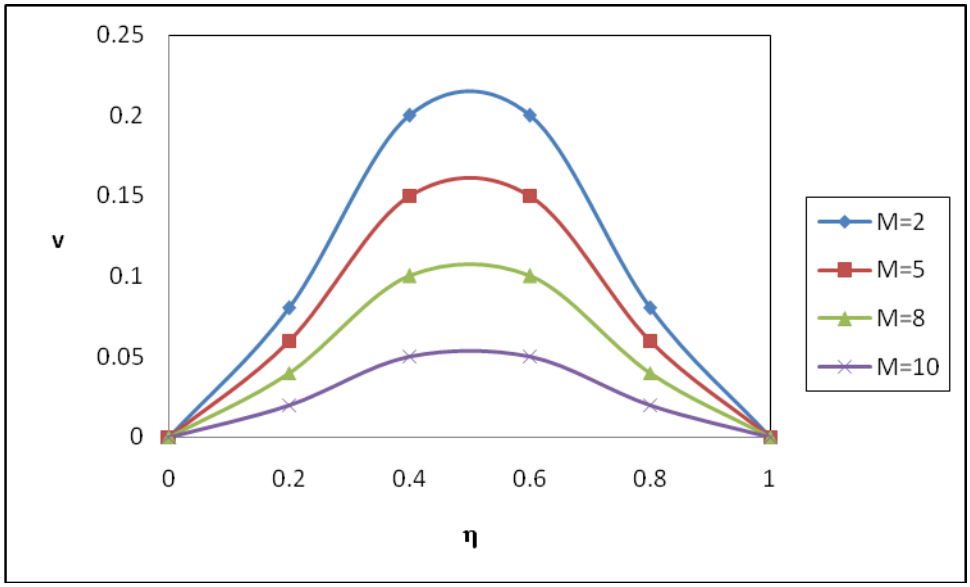

Figure 12: The velocity profile for *v* against M

k_1=1, *S*=1, D^{-1} =1000, *m*=1, $x = t = \frac{\pi}{4}$, *R*=10, $\delta = 0.01$

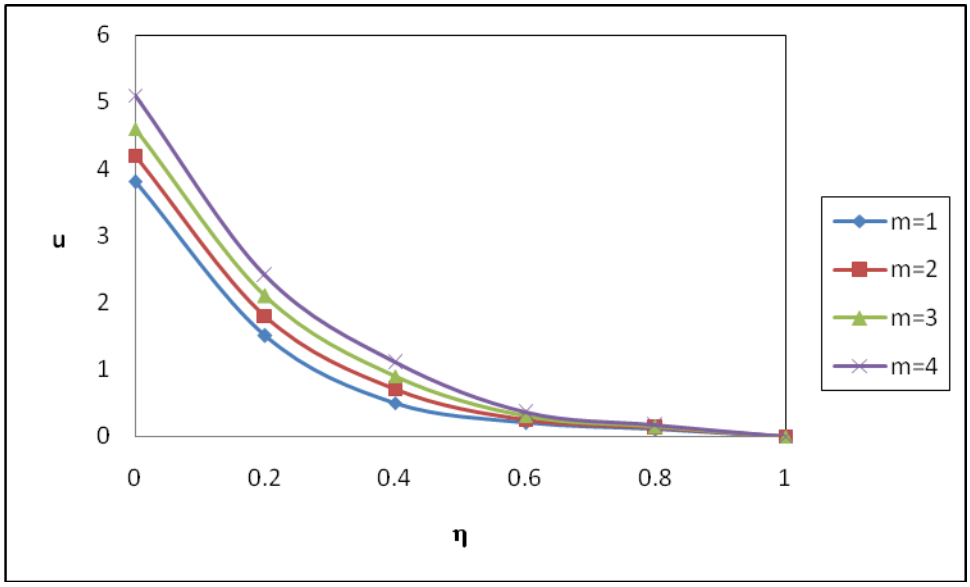

Figure 13: The velocity profile for *u* against *m*

k_1=1, *S*=1, D^{-1} =1000, *M*=2, $x = t = \frac{\pi}{4}$, *R*=10, $\delta = 0.01$

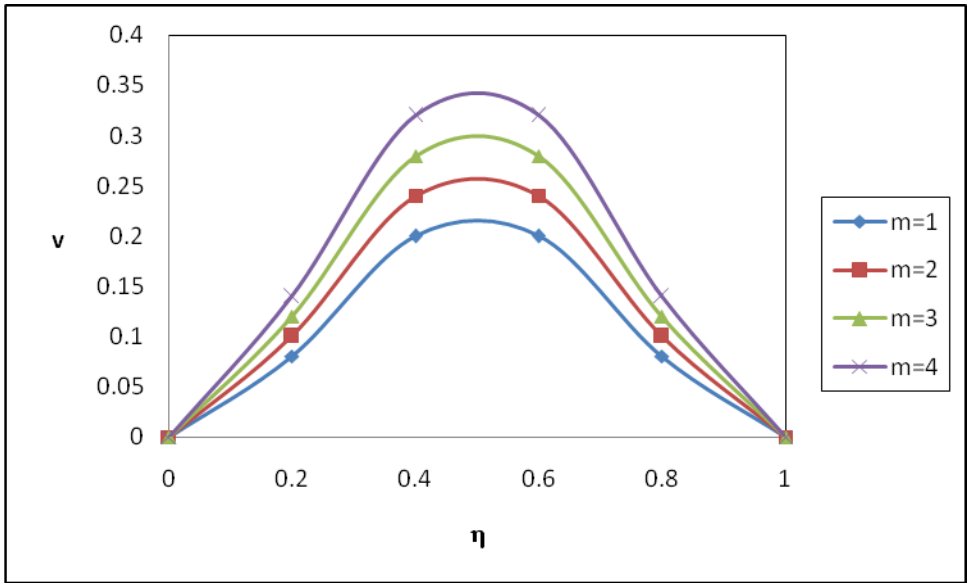

Figure 14: The velocity profile for *v* against *m*

k_1=1, *S*=1, D^{-1} =1000, *M*=2, $x = t = \frac{\pi}{4}$, *R*=10, $\delta = 0.01$

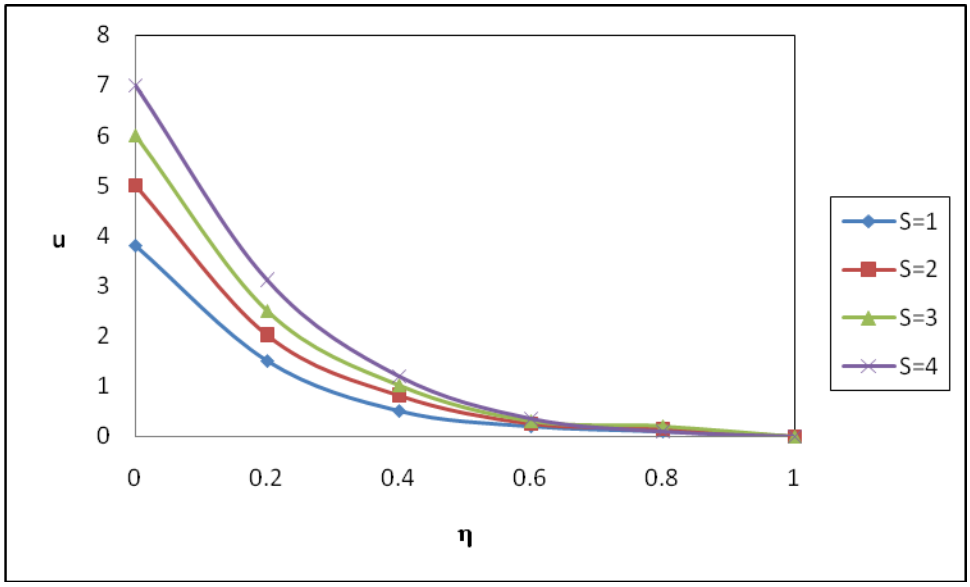

Figure 15: The velocity profile for *u* against *S*

k_1=1, D^{-1} =1000, M=2, m=1 $x = t = \frac{\pi}{4}$, R=10, $\delta = 0.01$

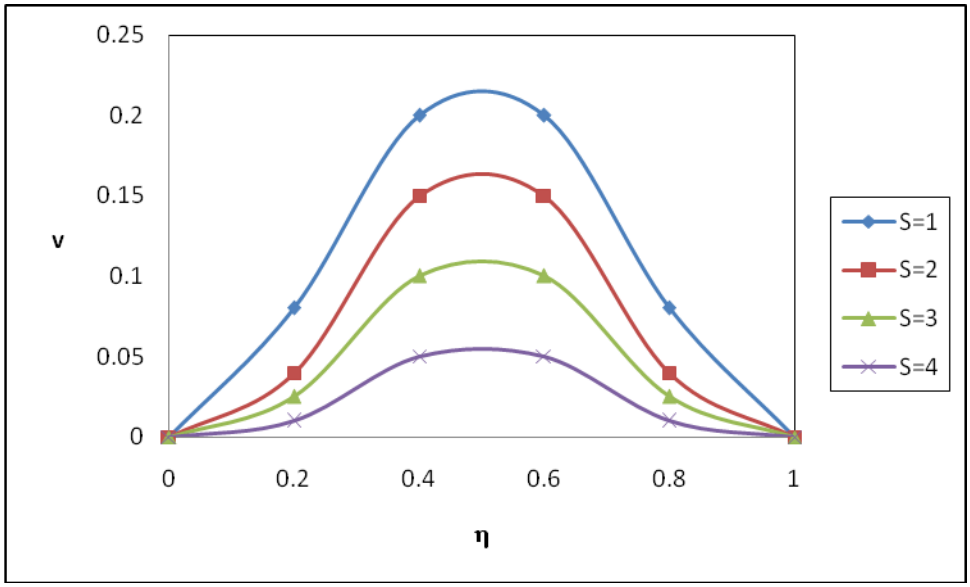

Figure 16: The velocity profile for *v* against *S*

k_1=1, D^{-1} =1000, M=2, m=1, $x = t = \frac{\pi}{4}$, R=10, $\delta = 0.01$

Table 1: The shear stress at the upper wall with S=1

x	I	II	III	IV	V	VI	VII	VIII	IX	X	XI	XII	XIII
0	2.9456	3.0045	3.1453	3.1145	3.2566	3.0835	3.1146	2.8145	2.7116	2.4653	2.0082	3.1566	3.1566
$\pi/4$	2.5675	2.6678	2.7566	2.6334	2.8346	2.6314	2.7366	2.4665	2.2265	2.1458	1.8113	2.8116	2.9958
$\pi/2$	2.1334	2.2469	2.3664	2.2883	2.3483	2.2108	2.3465	2.0065	1.8338	1.6652	1.2115	2.5665	2.8115
$3\pi/4$	3.4356	3.6678	3.6834	3.6836	3.7637	3.5289	3.6336	3.2115	3.0065	3.1148	2.8156	3.8314	4.2254
π	5.3114	5.3836	5.4266	5.4669	5.4995	5.4445	5.5333	5.1426	5.0083	5.1083	4.8309	5.9112	6.2318
$3\pi/2$	5.9445	5.9946	6.0053	6.3365	6.4143	6.1145	6.2225	5.7416	5.5783	5.6008	5.1245	6.5663	6.9665
$7\pi/4$	4.7866	4.8368	4.9014	4.9908	5.4652	5.6652	5.9863	4.4624	4.2211	5.5687	5.1833	4.9952	5.2336

.	I	II	III	IV	V	VI	VII	VIII	IX	X	XI	XII	XIII
R	10	30	50	10	10	10	10	10	10	10	10	10	10
D^{-1}	1000	1000	1000	2000	3000	1000	1000	1000	1000	1000	1000	1000	1000
K	1	1	1	1	1	1.5	2	1	1	1	1	1	1
δ	0.01	0.01	0.01	0.01	0.01	0.01	0.01	0.02	0.03	0.01	0.01	0.01	0.01
M	2	2	2	2	2	2	2	2	2	5	8	2	2
m	1	1	1	1	1	1	1	1	1	1	1	2	3

CONCLUSIONS

1. The resultant velocity also enhances with increasing the Reynolds parameter *R*.
2. Higher the permeability of the porous medium larger the axial velocity along the channel and rate of increase is sufficiently high. The resultant velocity reduces with increasing in the inverse Darcy parameter D^{-1}.
3. The resultant velocity increase with increasing the parameters k_1, x and *m*.
4. The resultant velocity also reduces with increasing the parameter δ.
5. The resultant velocity also decreases with increasing the Hartmann number *M*.
6. The magnitude of the axial velocity *u* enhances and the transverse velocity *v* reduces with increasing the oscillatory parameter *S*. The resultant velocity also enhances with increasing the oscillatory parameter *S*.
7. The shear stresses at the wall less than or equal to zero throughout the entire cycle of oscillation.
8. The influence of porosity in checking separation may be observed.
9. The shear stress on the upper wall does not vanish or become negative at any point in a wave length range throughout the entire cycle of oscillation.
10. The magnitude of the stresses enhances with increasing *R*, D^{-1}, k_1 , *x* and *m* and reduces with increasing δ and magnetic parameter *M* being fixed *S*.

REFERENCES

[1]. Latham TW, Fluid motion in a peristaltic pump, MIT Cambridge MA, 1966.

[2]. Shapiro AH, Jaffrin MY, Weinberg SL, Peristaltic pumping with long wavelengths at low Reynolds number. J. Fluid Mech. 1969; 37: 799–825.

[3]. Eldabe NTM, El-Sayed MF, Ghaly AY, Sayed HM, Peristaltically induced transport of a MHD biviscosity fluid in a non-uniform tube. Physica A. 2007; 383:253–266. doi: 10.1016/j.physa.2007.05.027

[4]. Noreen S, Hayat T, Alsaedi A, Qasim M, Mixed convection heat and mass transfer in the peristaltic flow with chemical reaction and inclined magnetic field. Indian Journal of Physics. 2013; 87:889–896. doi: 10.1007/s12648-013-0316-2

[5]. Noreen S, Ahmad B, Hayat T, Mixed Convection Flow of Nanofluid in Presence of an Inclined Magnetic Field. PloS One. 2013; 8:e73248.

doi: 10.1371/journal.pone.0073248 PMID: 24086276

[6]. Kothandapani M, Srinivas S, Peristaltic transport of a Jeffrey fluid under the effect of magnetic field in an asymmetric channel. Int. J. Non-Linear Mech. 2008; 43:915–924. doi: 10.1016/j.ijnonlinmec.2008. 06.009

[7]. Mehmood OU, Mustapha N, Shafie S, Peristaltically Induced Flow of Fourth Grade Fluid with Viscous Dissipation. WASJ. 2013; 21:36–141,.

[8]. Mehmood OU, Mustapha N, Shafie S, Heat transfer on peristaltic flow of fourth grade fluid in inclined asymmetric channel with partial slip. Appl. Math. Mech. -Engl. Ed. 2012; 33:1313–1328.

[9]. Tripathi D, Pandey SK, Das S, Peristaltic flow of viscoelastic fluid with fractional Maxwell model through a channel. Appl. Math. Comput. 2010; 215: 3645–3654.

[10]. Nowar K, Peristaltic flow of a nanofluid under the effect of Hall current and porous medium. Math. Prob. Engg. 2014; pii 389581 (15).

[11]. Hayat T, Ali N and Asghar S, Hall effects on peristaltic flow of a Maxwell fluid in a porous

medium. Physics Letters A. 2007; 363: 397–403.

doi: 10.1016/j.physleta.2006.10.104

[12]. Siddiqui AM, Rana MA, Ahmed N, Effects of hall current and heat transfer on MHD flow of a Burgers' fluid due to a pull of eccentric rotating disks. Communications in Nonlinear Science and Numerical Simulation. 2008; 13:1554–1570. doi: 10.1016/j.cnsns.2006.10.005 .

[13]. Gad NS, Effect of Hall currents on interaction of pulsatile and peristaltic transport induced flows of a particle-fluid suspension. Applied Mathematics and Computation. 2011; 217: 4313–4320. doi: 10.1016/j. amc.2010.08.016 .

[14]. Mekheimer KS, Elmaboud YA, The influence of heat transfer and magnetic field on peristaltic transport of a Newtonian fluid in a vertical annulus: Application of an endoscope. Phys. Lett. A 2008; 372: 1657–1665.

doi: 10.1016/j.physleta.2007.10.028 .

[15]. Mekheimer KS, Husseny SZA, Elmaboud YA, Effects of heat transfer and space porosity on peristaltic flow in a vertical asymmetric channel. Numer. Methods Partial Diff. Eqs. 2010; 26: 747–770.

[16]. Kothandapani M, Srinivas S, Peristaltic transport in an asymmetric channel with heat transfer–A note. Int. Comm. Heat Mass transfer 2008; 35: 514–522.

[17]. Kothandapani M, Srinivas S, The influence of heat and mass transfer on MHD peristaltic flow through a porous space with compliant walls. Appl. Math. Comput. 2009; 213: 197–208.

[18]. Kothandapani M, Srinivas S, Effects of chemical reaction and space porosity on MHD mixed convective flow in a vertical asymmetric channel with peristalsis. Math Comp. Mod. 2011; 54: 1213–1227.

[19]. Hayat T, Noreen S, Qasim M, Influence of heat and mass transfer on the peristaltic transport of PhanThien- Tanner fluid. ZNA. 2013; 68a:751–758.

[20]. Ogulu A, Effect of heat generation on low Reynolds number fluid and mass transport in a single lymphatic blood vessel with uniform magnetic field. Int. Comm. Heat Mass Transfer 2006; 33: 790–799.

[21]. Boger DV, Demonstration of upper and lower Newtonian fluid behavior in a pseudoplastic fluid. Nature 1977; 265:126–128. doi: 10.1038/265126a0 .

[22]. Hayat T, Noreen S, Alhothuali M, Asghar S, Alhomaidan A, Peristaltic flow under the effects of an induced magnetic field and heat and mass transfer. Int. J. Heat Mass Transf. 2012; 55:443–452.

doi: 10. 1016/j.ijheatmasstransfer.2011.09.044 .

[23]. Hayat T, Noreen S, Asghar S, Hendi A A, Influence of an induced magnetic field on peristaltic transport in an asymmetric channel. Chem. Engg. Commun. 2011; 198: 609–628. doi: 10.1080/00986445.2011. 53269

[24]. VeeraKrishna.M and M.Gangadhar Reddy, "MHD free convective rotating flow of Visco-elastic fluid past an infinite vertical oscillating porous plate with chemical reaction," IOP Conf. Series: Materials Science and Engineering 2016;149:012217 doi:http://dx.doi.org/10.1088/1757-899X/149/1/012217.

[25]. VeeraKrishna.M and G.Subba Reddy, "Unsteady MHD convective flow of Second grade fluid through a porous medium in a Rotating parallel plate channel with temperature dependent source," IOP Conf. Series: Materials Science and Engineering, 2016; 149: 012216 doi**:** http://dx.doi.org/10.1088/1757-899X/149/1/012216.

[26]. VeeraKrishna.M and B.V.Swarnalathamma, "Convective Heat and Mass Transfer on MHD Peristaltic Flow of Williamson Fluid with the Effect of Inclined Magnetic Field," AIP Conference Proceedings 1728 (2016):020461 doi: http://dx.doi.org/10.1063/1.4946512

[27]. Swarnalathamma. B. V. and M. Veera Krishna, "Peristaltic hemodynamic flow of couple stress fluid through a porous medium under the influence of magnetic field with slip effect, AIP Conference Proceedings 1728 (2016):020603 doi: http://dx.doi.org/10.1063/1.4946654

[28]. M.Veera Krishna, M.Gangadhar Reddy, MHD Free Convective Boundary Layer Flow through Porous medium Past a Moving Vertical Plate with Heat Source and Chemical Reaction, Materials Today: Proceedings, vol. 5, pp. 91–98, 2018. https://doi.org/10.1016/j.matpr.2017.11.058.

[29]. M.Veera Krishna, G.Subba Reddy, MHD Forced Convective flow of Non-Newtonian fluid through Stumpy Permeable Porous medium, Materials Today: Proceedings, vol. 5, pp. 175–183, 2018. https://doi.org/10.1016/j.matpr.2017.11.069.

[30]. M.Veera Krishna, Kamboji Jyotghi, Hall effects on MHD Rotating flow of a Visco-elastic Fluid through a Porous medium Over an Infinite Oscillating Porous Plate with Heat source and Chemical reaction, Materials Today: Proceedings, vol. 5, pp. 367–380, 2018. https://doi.org/10.1016/j.matpr.2017.11.094.

[31]. B. Siva Kumar Reddy, M. Veera Krishna , K.V.S.N. Rao, R. Bhuvana Vijaya, HAM Solutions on MHD flow of nano-fluid through saturated porous medium with Hall effects, Materials Today: Proceedings, vol. 5, pp. 120–131, 2018. https://doi.org/10.1016 /j.matpr.2017.11.062.